Available online at www.sciencedirect.com
SCIENCE DIRECT®
Thin Solid Films 496 (2006) 99 – 103
www.elsevier.com/locate/tsf

Electrical and optical properties of amorphous indium zinc oxide films

N. Ito [a,b], Y. Sato [a], P.K. Song [a,c], A. Kaijio [d], K. Inoue [d], Y. Shigesato [a,*]

[a] Graduate School of Science and Engineering, Aoyama Gakuin University, J410, 5-10-1 Fuchinobe Sagamihara, Kanagawa, 229-8558, Japan
[b] Advanced Technologies Fusion Laboratory Devices Research, Matsushita Electric Works, Ltd., 1048, Kadoma, Osaka, 571-8686, Japan
[c] School of Materials Science and Engineering, Pusan National University, Jangjeon-dong, Keumjung-ku, Pusan, 609-735, South Korea
[d] Idemitsu Kosan Co., Ltd., 1280 Kami-izumi Sodegaura, Chiba, 299-0293, Japan

Available online 28 September 2005

Abstract

Valence electron control and electron transport mechanisms on the amorphous indium zinc oxide (IZO) films were investigated. The amorphous IZO films were deposited by dc magnetron sputtering using an oxide ceramic IZO target (89.3 wt.% In_2O_3 and 10.7 wt.% ZnO). N-type impurity dopings, such as Sn, Al or F, could not lead to the increase in carrier density in the IZO. Whereas, H_2 introduction into the IZO deposition process was confirmed to be effective to increase carrier density. By 30% H_2 introduction into the deposition process, carrier density increased from 3.08×10^{20} to 7.65×10^{20} cm^{-3}, which must be originated in generations of oxygen vacancies or interstitial Zn^{2+} ions. Decrease in the transmittance in the near infrared region and increase in the optical band gap were observed with the H_2 introduction, which corresponded to the increase in carrier density. The lowest resistivity of 3.39×10^{-4} Ω cm was obtained by 10% H_2 introduction without substrate heating during the deposition.

Keywords: Indium zinc oxide; IZO; Amorphous; Transparent conductive oxide; Sputtering; Valence electron control

1. Introduction

Transparent conductive oxide (TCO) films have been widely used in the field of optoelectronic devices, such as transparent electrodes for various kinds of flat panel displays (FPDs) or photovoltaic devices [1–3]. With recent demands for the large-area and high-quality FPDs, amorphous transparent conductive films including amorphous Sn-doped In_2O_3 (ITO) films have attracted significant attention to their very flat surface, low internal stress and good etchability for micro-patterning. However, crystallinity of sputter deposited ITO films are reported to depend heavily on total gas pressure during the deposition and fully amorphous films could be deposited only at rather high total gas pressure of 3–5 Pa, when the substrate temperature (T_s) was around RT [4,5]. Inoue et al. reported that IZO films (In_2O_3/ZnO = 89.3:10.7 by wt.%) with entirely amorphous structure could be obtained with high reproducibility under the wide range of the deposition conditions such as total gas pressure or substrate temperature up to 300 °C, where the resistivity of the films was about $4–5 \times 10^{-4}$ Ω cm [6,7]. These amorphous IZO films were reported to have the smaller compressive stress and much smoother surfaces than the polycrystalline ITO films deposited under the same sputtering conditions [8]. Wet etching properties of the amorphous IZO films with optimized electrical properties were also reported to be superior to those of the polycrystalline ITO films since they could be etched easily with weak acid solution such as oxalic acid and formatted to the taper-shaped fine pitch pattern [7]. Therefore, the IZO is expected to be a new candidate for transparent electrode especially for thin film transistor (TFT)-LCDs or organic ELDs.

In this study the IZO films were deposited by dc magnetron sputtering which should be one of the most promising deposition techniques for the commercial uniform coatings in large area with high packing density and strong adhesion. The valence electron control in IZO was attempted and electron transport mechanisms were investigated.

2. Experimental details

The films were deposited on unheated non-alkali glass (AN100, Asahi Glass) or Si wafer substrates by dc magnetron

* Corresponding author. Tel.: +81 42 759 6223; fax: +81 42 759 6493.
E-mail address: yuzo@chem.aoyama.ac.jp (Y. Shigesato).

0040-6090/$ - see front matter © 2005 Elsevier B.V. All rights reserved.
doi:10.1016/j.tsf.2005.08.257

sputtering using the oxide ceramic In_2O_3–ZnO target (89.3 wt.% In_2O_3 and 10.7 wt.% ZnO, Idemitsu Kosan Co., Ltd.). Substrate temperature during the deposition was confirmed to be lower than 50 °C by the thermo-label. Total gas pressure (P_{tot}) of Ar or Ar+H_2 was kept at 0.5 Pa for all the depositions. Water partial pressure of the residual gas was maintained to be less than 8×10^{-4} Pa, which was monitored using a quadrupole mass spectrometer (Transpector XPR2, Inficon), in order to guarantee high reproducibility of the film properties. Valence electron control was tried by the following two methods, (a) impurity dopings, such as Sn, Al and F, or (b) H_2 gas introduction into the IZO deposition process in order to generate oxygen vacancies or interstitial Zn^{2+} ions by slight reduction. The Sn or Al dopings were carried out by placing each oxide pellets at the erosion area of the target surface, whereas the F doping were carried out by introducing CF_4 gas during the deposition which was confirmed to be effective for the F doping of polycrystalline In_2O_3 [9]. The thickness of all the films in this study was adjusted to be about 200 nm by controlling deposition time.

The film thickness was measured using a surface profiler (Dektak^3, Sloan Tech.). Resistivity (ρ), Hall mobility (μ) and free carrier density (n) of the films were measured by the four-point probe method and Hall-effect measurement in the van der Pauw geometry (HL-550PC, Bio-Rad). For the IZO film with optimized electrical properties, the temperature dependence of resistivity, Hall mobility and carrier density was measured over a temperature range from 90 to 500 K. X-ray diffraction (XRD) was carried out by 40 kV, 20 mA $CuK_{\alpha 1}$ radiation (XRD-6000, Shimadzu). Surface morphology of the films was analyzed by atomic force microscopy (AFM, SPM-9500, Shimadzu). Transmittance and reflectance of the films were measured from 300 to 2600 nm using a spectrophotometer (UV-3100, Shimadzu).

3. Results and discussion

Fig. 1 shows XRD patterns of the IZO films deposited under 100% Ar gas without substrate heating and post-annealed in air at 100–500 °C for 1 h. The XRD profiles of the as-deposited film and post-annealed films at l00–400 °C showed halo pattern at around $2\theta = 30–35°$, implying that all these films were entirely amorphous. The film post-annealed at 500 °C showed In_2O_3 polycrystalline structure, indicating that crystallization temperature of the IZO films was between 400 and 500 °C in air. The crystallization temperatures of amorphous In_2O_3 or ITO films have been reported to be 160–170 °C or 170–180 °C, respectively [10,11], so it can be said that the amorphous IZO films are more thermally stable than the amorphous In_2O_3 or ITO films. These IZO films were found to have a very smooth surface of Ra=0.2 nm analyzed by AFM, whereas the polycrystalline ITO and GZO films were reported to have a rougher surface of Ra=0.8–1.6 nm.

Fig. 2 shows (a) resistivity, ρ, (b) Hall mobility, μ and (c) carrier density, n of the IZO films as-deposited (open triangle) and post-annealed for 1 h at various temperatures in vacuum (6×10^{-4} Pa) (open square) and post-annealed in air (closed square), respectively. After the post-annealing in air, resistivity

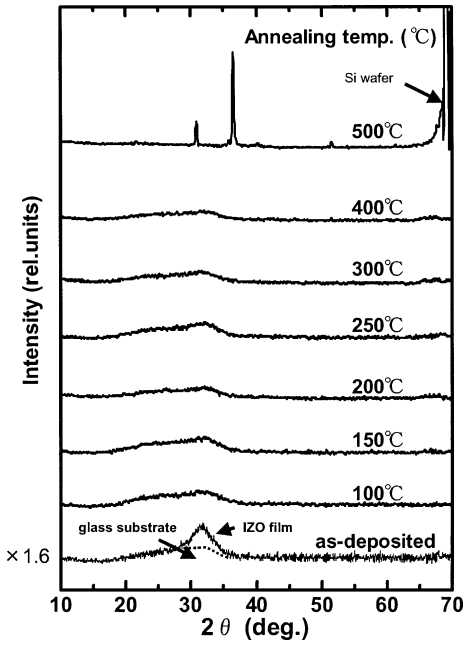

Fig. 1. XRD pattern of the IZO film deposited in 100% Ar gas without substrate heating and post-annealed at various temperatures for 1 h in air. The films were deposited on non-alkali glass, except for the films of the 500 °C annealing for which Si wafer was used as substrate.

increased drastically at higher than 150 °C, which can be attributed to the decrease in carrier density. On the other hand, in the case of the post-annealing in vacuum, resistivity remained relatively constant, where carrier density was almost constant. The decrease in carrier density by the post-annealing in air must be caused by the extinction of oxygen vacancies or interstitial Zn^{2+} ions, implying that carrier density of the amorphous IZO films should be mainly dominated by the oxygen vacancies or interstitial Zn^{2+} ions.

Fig. 3 shows the variation in (a) resistivity, (b) Hall mobility and (c) carrier density of the IZO films deposited with the H_2 introduction at various $H_2/(Ar+H_2)$ flow ratios (R_{H_2}) of 0–50%. All these films were also confirmed to show only halo pattern in XRD and to have amorphous structure. The systematic increase in carrier density from 3.08×10^{20} to 7.65×10^{20} cm^{-3} with the increase in R_{H_2} from 0 to 30% was clearly observed. The lowest resistivity of 3.39×10^{-4} Ω cm was obtained at $R_{H_2}=10\%$. The H_2 introduction into the IZO deposition process was confirmed to be effective in order to increase carrier density. On the other hand, the n-type impurity dopings of cations or anion, such as Sn^{4+} for In^{3+}, Al^{3+} for Zn^{2+}, or F^- for O^{2-}, by 0.1–3.0% could not lead to the increase in carrier density in the IZO. These results correspond to the reports that the doped Sn could not be electrically active in the amorphous ITO films, where the doped Sn became electrically active and released free electrons after the crystallization [11,12].

Fig. 4 shows transmittance and reflectance from 300 to 2600 nm for the IZO films deposited with the H_2 introduction ($R_{H_2}=0$, 10% and 30%) at P_{tot} of 0.5 Pa. For the films deposited at larger R_{H_2}, transmittance in near-infrared region of wavelength larger than 1000 nm decreased, where reflectance increased. This behavior is caused by the increase in plasma

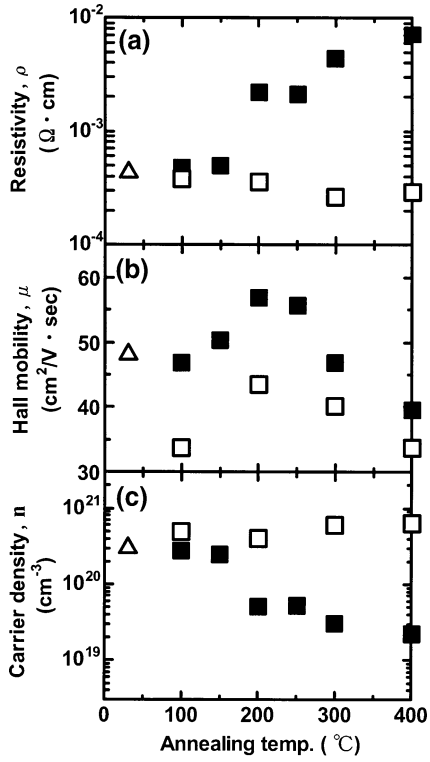

Fig. 2. (a) Resistivity, ρ, (b) Hall mobility, μ and (c) carrier density, n of the IZO films as-deposited (open triangle) and post-annealed for 1 h at various temperatures in vacuum ($6\times10^{-}$super ^{4} Pa) (open square) and post-annealed in air (closed square), respectively.

oscillation frequency with the increasing carrier density, which could be explained quantitatively by Drude theory and is well known in degenerated TCO films [13,14]. Optical constants of

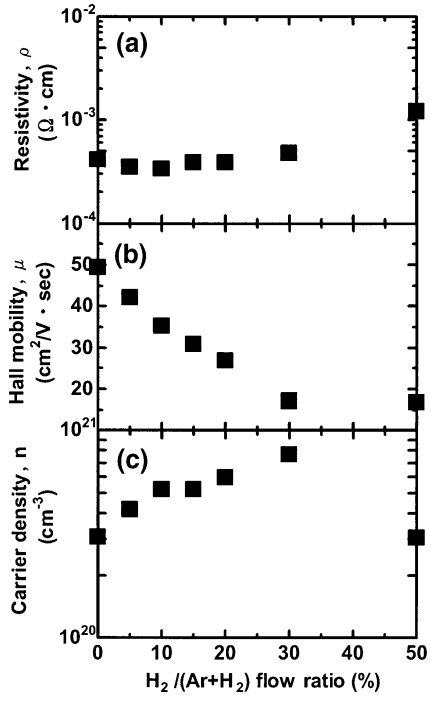

Fig. 3. (a) Resistivity, (b) Hall mobility and (c) carrier density of the IZO films deposited at P_{tot}=0.5 Pa with the H_2 introduction at various $H_2/(Ar+H_2)$ flow ratios (R_{H_2}) of 0–50%.

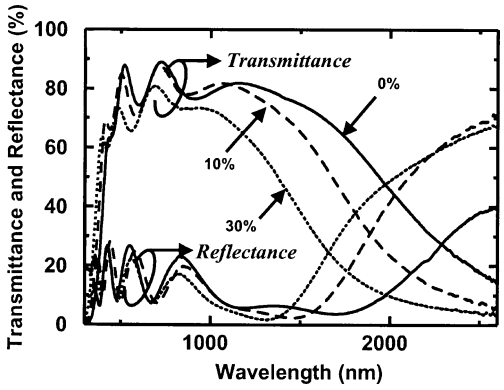

Fig. 4. Transmittance and reflectance from 300 to 2600 nm for the IZO films deposited at P_{tot}=0.5 Pa with the H_2 introduction at various $H_2/(Ar+H_2)$ flow ratios (R_{H_2}) of 0, 10% and 30%.

refractive index (n_{op}) and extinction coefficient (k) were estimated by Newton-Raphson's method from the transmittance and reflectance spectra in near-ultraviolet region. From the value k, the absorption coefficient α can be derived by

$$\alpha = 4\pi\, k/\lambda.$$

It is commonplace to use a relation

$$\alpha \propto \left(\hbar\omega - E_g\right)^{1/2} \text{ for } \hbar\omega > E_g$$

to obtain optical band gap (E_g) for highly degenerated oxide semiconductors based on the assumption of direct allowed transitions to an empty parabolic conduction band [13,14]. α^2 is plotted as a function of the photon energy ($\hbar\omega$) in Fig. 5. E_g are extrapolated to increase from 3.48 to 3.84 eV by increasing R_{H_2} from 0 to 30%. This increase in E_g can be explained by Burstein-Möss (BM) effect in which the lowest states in the conduction band are blocked and transitions can take place only to energies above Fermi level. Thus the optical constants both in the near-ultraviolet and near-infrared regions implied the increase in n with the introduction of H_2 during the deposition. As a consequence, both the electrical and optical analyses indicate that the introduction of H_2 is effective to generate oxygen vacancies or interstitial Zn^{2+} ions, and hence increase the carrier density of the amorphous IZO films.

Fig. 6 shows the electrical properties of the IZO film deposited with the H_2 introduction at R_{H_2}=10% in the

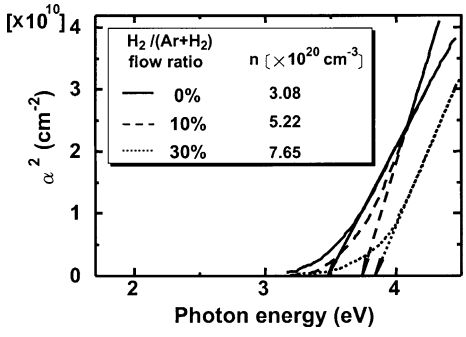

Fig. 5. The square of absorption coefficient (α^2) of the IZO films deposited at P_{tot}=0.5 Pa with the H_2 introduction at various $H_2/(Ar+H_2)$ flow ratios (R_{H_2}) of 0, 10% and 30%, as a function of the photon energy (eV).

temperature ranging from 500 to 90 K. The mobility, carrier density and resistivity were almost constant, which corresponded with the typical electrical properties of highly degenerated TCO films [14]. Generally the cause of scattering of carriers which dominates the mobility in degenerated TCO films has been considered to be the following factors, i.e., ionized impurities, neutral impurities, grain boundaries, lattice vibrations, and dislocations. As shown in Fig. 6, mobility was almost constant in this temperature range, implying that lattice vibration scattering or dislocation scattering might be unimportant. In addition, since the IZO films are completely amorphous structure, electron scattering at grain boundaries should also have little importance. The contribution of ionized scattering centers using Fermi-Dirac distribution function has been previously described by the following Brook-Herring-Dingle (BHD) theory [12,14–16],

$$\mu_{\mathrm{I}} = \frac{24\pi^3(\varepsilon_0\varepsilon_r)^2\hbar^3 n}{e^3 m^{*2} g(x) Z^2 n_{\mathrm{I}}}, \tag{1}$$

where the scattering function $g(x)$ is given by

$$g(x) = \ln\left(1+\frac{4}{x}\right) - \frac{1}{\left(1+\frac{x}{4}\right)}$$

and

$$x = \frac{e^2 m^*}{\pi\varepsilon_0\varepsilon_r\hbar^2\sqrt[3]{3\pi^5 n}}.$$

Here ε_0 and ε_r are the dielectric constant of free space and relative permittivity. Z and n_1 are the charge and the density of the ionized scattering centers, respectively. The values of the effective mass, m^* and dielectric constant, ε_r were selected from the ITO literature: a value of $0.3m_e$ was used for m^* and 9 for ε_r [12–14]. The calculated μ_I using Eq. (1) is plotted as a function of n in Fig. 7 by the assumption that the carrier density is due entirely to oxygen vacancies (dotted line). The mobility values of all the IZO films obtained in this study are also plotted in Fig. 7. In the case of the as-deposited IZO films using only Ar sputter gas, the mobility showed slightly smaller value than μ_I implying that electron scattering should mainly be dominated by the ionized impurity. The other IZO films showed roughly similar tendency, however some films have much smaller mobility than μ_I. This might be explained by electron scattering also by the neutral scattering centers similar to those already reported for ITO films [12,14].

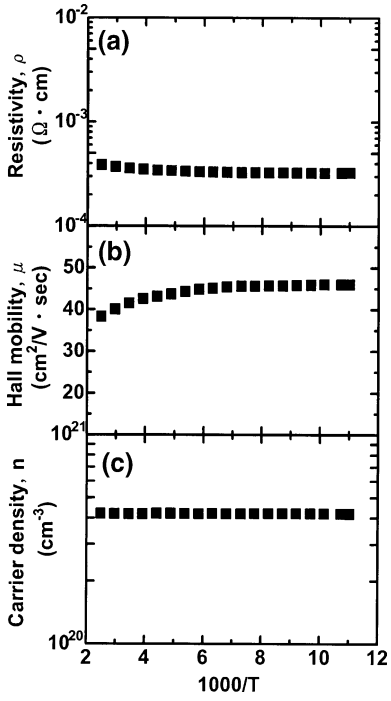

Fig. 6. (a) Resistivity, (b) Hall mobility and (c) carrier density of the IZO film deposited at P_{tot}=0.5 Pa with the H_2 introduction at $H_2/(Ar+H_2)$ flow ratio (R_{H_2}) of 10% in relation to the temperature from 500 to 90 K.

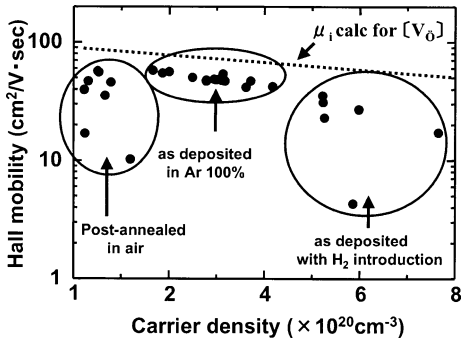

Fig. 7. Mobility vs. carrier density of the IZO films prepared under various deposition conditions or post-annealing conditions. The calculated mobility (μ_I) based on the BHD theory with the assumption that all the scattering centers of the free carriers are doubly charged oxygen vacancies ($V_{\ddot{o}}$) is also shown by dotted line.

4. Conclusion

Amorphous IZO films were deposited on unheated substrates by dc magnetron sputtering using the oxide ceramic In_2O_3–ZnO target. Valence electron control on the IZO films was investigated in order to increase carrier density. The carrier density was successfully increased from 3.08×10^{20} to 7.65×10^{20} cm^{-3} by introducing H_2 gas ($H_2/(Ar+H_2)$=30%) into the sputter deposition process. The IZO film with the lowest resistivity of 3.39×10^{-4} Ω cm was obtained for H_2 gas flow ratio of 10%. Decrease in the transmittance in the near infrared region and increase in optical band gap were observed with the introduction of H_2 gas ($H_2/(Ar+H_2)$=0–30%), which corresponds to the increase in the carrier density. As a consequence the H_2 gas introduction should be effective to generate oxygen vacancies or interstitial Zn^{2+} ions, and hence increased the carrier density of the amorphous IZO films. Electron transport mechanisms of the IZO films were considered to be dominated mainly by ionized scattering centers and neutral scattering centers.

Acknowledgements

This work was partially supported by a Grant-in-Aid for the 21st COE Program from the Ministry of Education, Culture,

Sports, Science and Technology (MEXT) of the Japanese Government.

References

[1] H. Koh, K. Sawada, M. Ohgawara, T. Kuwata, M. Akatsuka, M. Matsuhiro, SID Dig. Tech. Pap. 19 (1988) 53.
[2] T. Tsutsui, Oyobuturi 66 (2) (1997) 109, (in Japanese).
[3] H. Kobayashi, Y. Ishida, Y. Nakato, H. Tsubomura, J. Appl. Phys. 69 (1991) 1736.
[4] P.K. Song, Y. Shigesato, M. Kamei, I. Yasui, Jpn. J. Appl. Phys. 38 (1999) 2921.
[5] P.K. Song, Y. Shigesato, I. Yasui, C.W. Ow-Yang, D.C. Paine, Jpn. J. Appl. Phys. 37 (4) (1998) 1870.
[6] K. Inoue, Kinou zairyou 19 (9) (1999) 39, (in Japanese).
[7] A. Kaijyo, K. Inoue, S. Matsyzaki, Y. Shigesato, Proceedings for the 4th Pacific Rim International Conference on Advanced Materials and Processing (PRICM-4), vol. 2, 2001, p. 1787.
[8] T. Sasabayashi, N. Ito, M. Kon, P.K. Song, K. Ustumi, A. Kajio, Y. Shigesato, Thin Solid Films 445 (2003) 219.
[9] Y. Shigesato, N. Shin, M. Kamei, P.K. Song, I. Yasui, Jpn. J. Appl. Phys. 39 (2000) 6422.
[10] C.W. Ow-Yang, D. Spinner, Y. Shigesato, D.C. Paine, J. Appl. Phys. 83 (1) (1998) 145.
[11] M. Kamei, H. Akao, P.K. Song, I. Yasui, Y. Shigesato, Korean Ceram. Soc. 6 (2) (2000) 107.
[12] Y. Shigesato, D.C. Paine, Appl. Phys. Lett. 62 (11) (1993) 1268.
[13] I. Hamberg, C.G. Granqvist, J. Appl. Phys. 60 (1986) R123.
[14] Y. Shigesato, D.C. Paine, T.E. Haynes, J. Appl. Phys. 73 (1993) 3805.
[15] R.B. Dingle, Philos. Mag. 46 (1955) 831.
[16] R. Clanget, Appl. Phys. 2 (1973) 247.